Langmuir

Article

pubs.acs.org/Langmuir

Self-Assembly Behavior of Alkylated Isophthalic Acids Revisited: Concentration in Control and Guest-Induced Phase Transformation

Kwang-Won Park,[†,‡] Jinne Adisoejoso,*[,†] Jan Plas,[†] Jongin Hong,[‡] Klaus Müllen,[§] and Steven De Feyter*[,†]

[†]Division of Molecular Imaging and Photonics, Department of Chemistry, Katholieke Universiteit Leuven, Celestijnenlaan 200 F, 3001 Leuven, Belgium

[‡]Laboratory of Nano-Materials Chemistry, Department of Chemistry, Chung-Ang University, Seoul 156-756, Republic of Korea

[§]Max-Planck Institute for Polymer Research, Ackermannweg 10, D-55128 Mainz, Germany

Supporting Information

ABSTRACT: The engineering of two-dimensional crystals by physisorption-based molecular self-assembly at the liquid−solid interface is a powerful method to functionalize and nanostructure surfaces. The formation of high-symmetry networks from low-symmetry building blocks is a particularly important target. Alkylated isophthalic acid (ISA) derivatives are early test systems, and it was demonstrated that to produce a so-called porous hexagonal packing of plane group *p*6, i.e., a regular array of nanowells, either short alkyl chains or the introduction of bulky groups within the chains were mandatory. After all, the van der Waals interactions between adjacent alkyl chains or alkyl chains and the surface would dominate the ideal hydrogen bonding between the carboxyl groups, and therefore, a close-packed lamella structure (plane group *p*2) was uniquely observed. In this contribution, we show two versatile approaches to circumvent this problem, which are based on well-known principles: the "concentration in control" and the "guest-induced transformation" methods. The successful application of these methods makes ISA suitable building blocks to engineer a porous pattern, in which the distance between the pores can be tuned with nanometer precision.

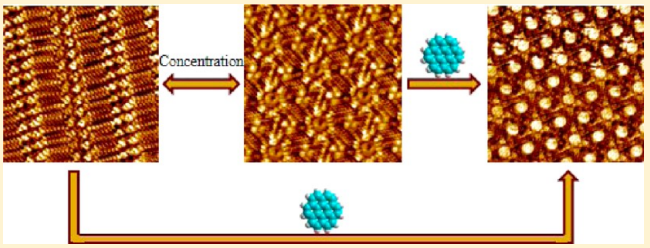

INTRODUCTION

Surface confined two-dimensional (2D) crystals consisting of molecular building blocks have garnered a broad interest in nanoscience because of their potential applications.[1−4] Traditionally, non-covalent interactions are used to guide the self-assembly process. Using hydrogen bonding,[5−8] van der Waals interactions,[9−12] metal−ligand coordination,[13−15] or a combination thereof as a molecular "glue", a multitude of architectures have been successfully engineered both in ultrahigh-vacuum conditions as well as at a liquid−solid interface. Predicting the specific outcome of network formation based on the molecular building blocks remains a challenge because various experimental factors govern the self-assembly process; solute concentration,[10,16−20] temperature,[21−25] and solvent[26,27] have all been known to influence the 2D crystal formation under ambient conditions.

It has previously been reported that alkylated isophthalic acid (ISA) derivatives show a variety of self-assembly motifs at the liquid/highly oriented pyrolytic graphite (HOPG) interface, where the outcome is determined by changes of the alkyl chains.[28−30] The main driving force for self-assembly was expected to be the intermolecular interaction between carboxylic groups in *meta* position, which, after dimerization through hydrogen bonding, could potentially yield linear zigzag or hexameric structures. It turned out, however, that ISA derivatives with a simple linear alkyl chain uniquely formed a lamellar structure, in which the intermolecular van der Waals interactions between adjacent interdigitated alkyl chains as well as the interaction between the chains and the underlying graphite dominate the hydrogen bonding. This forces the structure to circumvent ideal hydrogen bond formation. Only by significantly reducing the alkyl chain length and thereby lowering the impact of van der Waals interactions in favor of hydrogen bonding, cyclic hexameric structures were obtained.[29] As an alternative approach, the introduction of bulky groups at the end of the alkyl tails, which prevent ideal alkyl chain interdigitation, also produced hexameric structures.[28]

In this work, we show two simple approaches to create 2D nanoporous hexameric patterns at the liquid−solid interface using alkylated ISA derivatives without any inherent structural modifications of the building blocks, which are based on two well-known principles: "concentration in control"[16] and "guest-induced transformation".[31]

Received: October 15, 2014
Revised: November 24, 2014
Published: November 24, 2014

   dx.doi.org/10.1021/la5040849 | *Langmuir* 2014, 30, 15206−15211

RESULTS AND DISCUSSION

Concentration in Control. Three ISA derivatives [5-decyloxy-isophthalic acid (ISA-OC10), 5-tetradecyloxy-isophthalic acid, (ISA-OC14), and 5-octadecyloxy-isophthalic acid (ISA-OC18)], which differ only in the length of the alkyl chains, were chosen (Scheme 1), and their 2D self-assembly behavior at the liquid−solid interface was explored by scanning tunneling microscopy (STM). These molecular building blocks have two intrinsic recognition sites for noncovalent interactions: the alkyl chains give rise to van der Waals interactions through interdigitation, and the carboxylic acid groups form hydrogen bonds. Dependent upon the solute concentration used, ISA-OC10 and ISA-OC14 form a mixture of two distinct polymorphs, linear and porous, upon adsorption at the 1-phenyloctane/HOPG interface, while ISA-OC18 yields only the linear polymorph (see Figures S2−S4 of the Supporting Information). Figure 1 shows high-resolution STM images of the linear and porous polymorphs formed by ISA-OC14. At a relatively high concentration, a lamellar structure is predominantly observed for all three derivatives, similar to what has been reported earlier.[28,29] Within this lamellar structure, the van der Waals interactions clearly dominate the hydrogen-bond formation and force the molecules into a close packed *p*2 structure. The aromatic ISA headgroups appear as bright circles. On the basis of the STM contrast, it was impossible to determine the exact orientation or nature of the hydrogen bonds between the ISA headgroups; however, because of their head-to-head orientation (blue line in Figure 1a), dimer formation between the carboxylic acid

Scheme 1. (Left) Molecular Structure of ISA-OC*n* Molecules, where *n* = 9 for ISA-OC10, *n* = 13 for ISA-OC14, and *n* = 17 for ISA-OC18 and (Right) Molecular Structure of Coronene

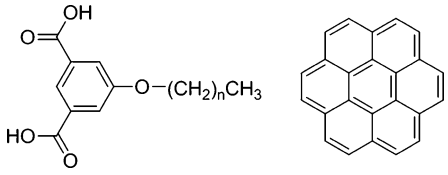

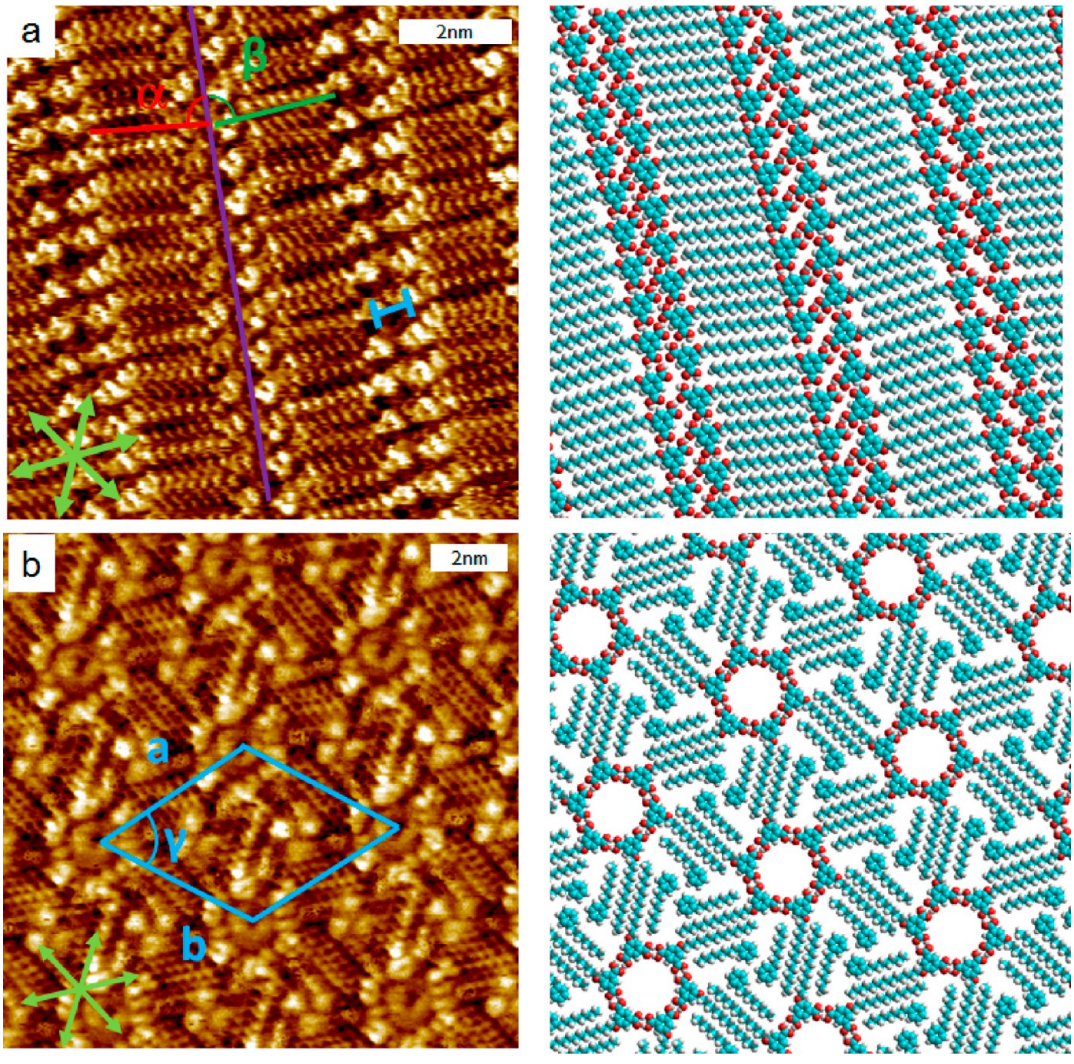

Figure 1. STM images and corresponding tentative molecular models of ISA-OC14 at the 1-phenyloctane/HOPG interface (0.52 mM; V_{bias} = 0.55 V; and I_{set} = 0.13 nA), showing (a) linear *p*2 network (α and β indicate the angle between the alkyl chains and the lamella axis) and (b) hexameric porous *p*6 phase (γ = 61° ± 4°; a = 4.00 ± 0.2 nm; and b = 4.30 ± 0.1 nm). The blue line indicates the distance between adjacent aromatic parts of ISA molecules. HOPG lattice vectors are indicated in green.

dx.doi.org/10.1021/la5040849 | *Langmuir* 2014, 30, 15206−15211

functionalities can be excluded.[32] It remains uncertain, however, how the ISA headgroups interact, therefore, only tentative models are given in Figure 1a and Figure S1 of the Supporting Information. The angle between the lamella axis and the alkyl chains is 90° ± 1° for ISA-OC18, while for ISA-OC14 (α = 84° ± 1°, and β = 86° ± 1°; Figure 1a) and ISA-OC10 (α = 78° ± 1°, and β = 86° ± 1°; see Figure S1 of the Supporting Information) two distinct orientations are observed. While, for ISA-OC18, all alkyl chains are oriented parallel to one of the main symmetry axes of HOPG, only the alkyl chains following the β angle (between lamella axis and the alkyl chains) are parallel to the main symmetry axis of HOPG.[33] This disparity can be understood as follows: relatively shorter alkyl chains give rise to a smaller contribution of van der Waals interactions to the structure formation, and the hydrogen bonds are therefore playing a more important role. However, the former still remains the dominant driving force for self-assembly. Bernasek *et al.* estimated the energy contributions of hydrogen-bond formation and van der Waals interaction in the lamellar structure of ISA-OC10 and ISA-OC18.[29] They confirmed that the share of hydrogen bonds (30-50 kJ/mol for both ISA-OC10 and ISA-OC18) increases as the share of the van der Waals interaction decreases with shorter alkyl chains (108−126 kJ/mol for ISA-OC18 to 60−70 kJ/mol for ISA-OC10).

Coexisting with the lamellar structure, ISA-OC10 and ISA-OC14 also form a hexameric porous *p6* structure at higher concentrations, which is phase-separated from the lamellar network. Lowering the solute concentration leads to the unique formation of this hexameric porous structure for ISA-OC10 and ISA-OC14 (see Figure S1 of the Supporting Information and Figure 1b, respectively), while the lamellar structure of ISA-OC18 seems to be unaffected by the solute concentration; it is still uniquely observed. Unlike the lamellar structure, within the hexameric structure, the hydrogen bonding is the dominant intermolecular interaction and the system adapts ideal hydrogen-bond formation, i.e., the dimer formation between adjacent carboxylic acids as observed previously in the case of non-alkylated ISA[34] and structurally related trimesic acids.[32] The hydrogen-bonded hexagonal pores are in their turn surrounded by six triangular pores, formed by van-der-Waals-mediated alkyl chain interdigitation. After close inspection, it was found that, for ISA-OC14, three phenyloctane solvent molecules reside in the triangular pores, identified by their bright aromatic headgroups.[35] Co-adsorption of these solvent molecules compensates for the loss in stability because of the large unoccupied areas in the triangular pores. Within the hexameric structure of ISA-OC10, the triangular pores become too small for solvent co-adsorption and appear featureless. This explains why the decrease of the hexameric structure coverage with an increasing concentration happens much faster for ISA-OC10 with respect to ISA-OC14. Decreasing the alkyl chain length maintains the hexagonal pore diameter constant (1.13 ± 0.1 nm) while decreasing the area of the triangular pores or, in other words, decreasing the distance between adjacent hexagonal pores.

The dependence of the surface coverage of the porous polymorph upon the concentration of ISA in solution is shown in Figure 2.[36] As seen from the graph, for both ISA-OC10 and ISA-OC14, the porous hexameric structure can be homogeneously engineered using a sufficiently low concentration. Surprisingly, even at the lowest concentration probed (0.01 mM), ISA-OC18 still exclusively forms the lamellar network,

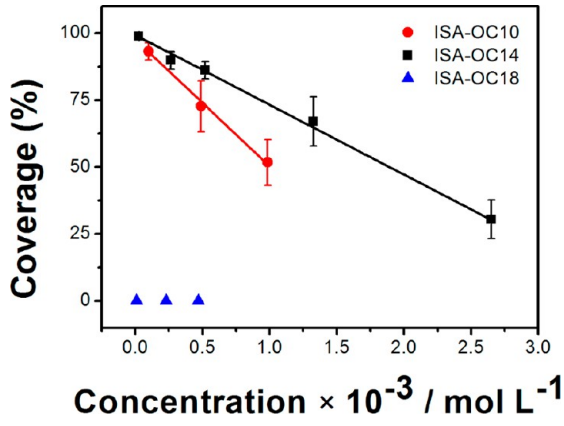

Figure 2. Dependence of the surface coverage of the porous structure upon the ISA concentration in solution. For each concentration, typically 10−15 large-scale images (100 × 100 nm) were recorded at different locations to be statistically relevant (see Figure S3 of the Supporting Information).

even though the surface coverage becomes sub-monolayer (see Figure S4 of the Supporting Information).

The concentration dependency of ISA derivatives is in good agreement with what has been observed earlier with similar molecular building blocks.[16] Traditionally, systems that are sensitive toward concentration consist of building blocks that are able to form two or more polymorphs with different adsorption energy and/or packing density. For ISA-OC10 and ISA-OC14, the packing density of the lamellar structure (1.23 molecules/nm^2 for ISA-OC10 and 0.69 molecules/nm^2 for ISA-OC14) and the hexameric structure (0.48 molecules/nm^2 for ISA-OC10 and 0.33 molecules/nm^2 for ISA-OC14) differs significantly. Therefore, at high concentrations, the number of molecules exceeds the amount required to cover the surface through hexameric structures and the system reacts by forming the close-packed lamella structure, using van der Waals forces between alkyl chains as the dominant driving force. However, at lower concentrations, less molecules are present at the interface and the system will react by forming the low-density network and allowing hydrogen-bond formation to dictate the structure. In comparison to ISA-OC10 and ISA-OC14, the difference in packing density between lamella and hexamers of ISA-OC18 is even larger. However, the energy penalty induced by the uncovered area of the triangular pores is simply too large, and therefore, even at sub-monolayer coverage, the formation of lamellae of ISA-OC18 is uniquely observed (see Figure S4 of the Supporting Information).

Guest-Induced Transformation. One of the main applications for nanoporous systems is the selective trapping of guest molecules in a spatially resolved manner. Moreover, apart from simple co-adsorption, it has been well-documented that the addition of guest molecules can overcome the energy loss caused by unoccupied areas, thereby templating the formation of a specific network.[31,37−39] Because non-alkylated ISA has been successfully applied to host coronene (COR), COR was chosen as the guest for the alkylated ISA host network.[34]

Upon premixing COR and the alkylated ISA derivatives in a 1:1 molar ratio (1:0.98 mM COR/ISA-OC10, 3:2.65 mM COR/ISA-OC14, and 0.5:0.47 mM COR/ISA-OC18), the hexameric structure is exclusively observed for all three derivatives (panels a−c of Figure 3). The COR molecules

dx.doi.org/10.1021/la5040849 | *Langmuir* 2014, 30, 15206−15211

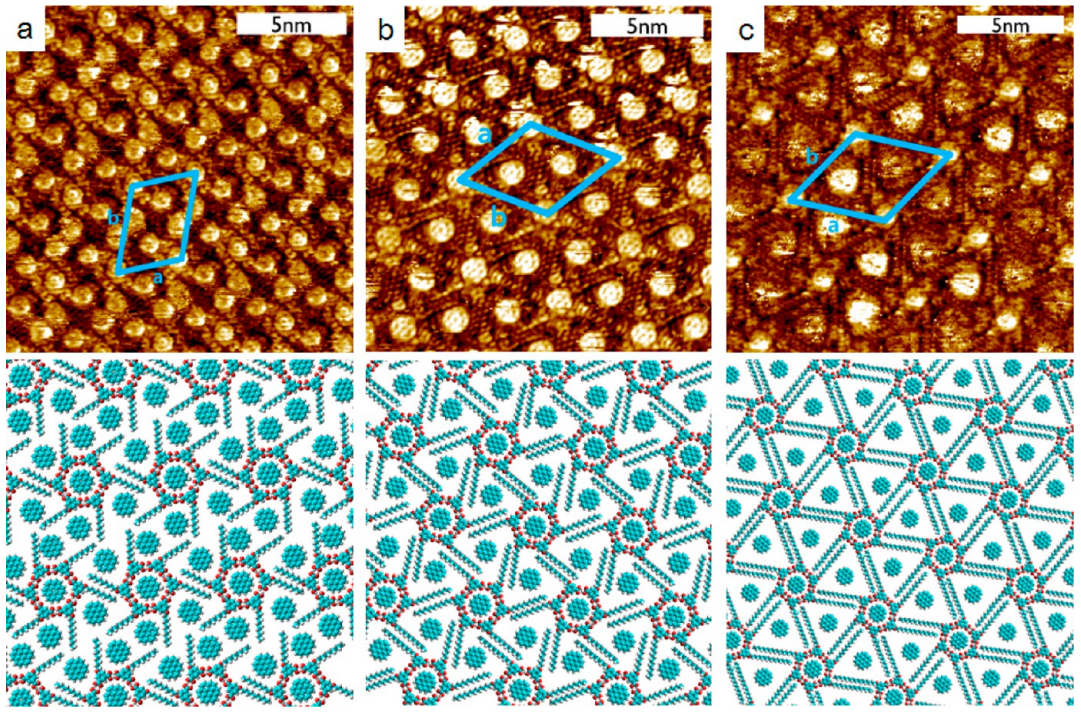

Figure 3. STM images and corresponding tentative models of a mixture of COR and (a) ISA-OC10, (b) ISA-OC14, and (c) ISA-OC18 in a 1:1 ratio (1:0.98 mM COR/ISA-OC10, 3:2.65 mM COR/ISA-OC14, and 0.5:0.47 mM COR/ISA-OC18). Unit cell parameters are (a) $\alpha = 68.6° \pm 1.3°$, $a = 3.24 \pm 0.1$ nm, and $b = 4.64 \pm 0.3$ nm; (b) $\alpha = 59.8° \pm 2.5°$, $a = 3.58 \pm 0.1$ nm, and $b = 3.66 \pm 0.1$ nm; and (c) $\alpha = 59.0° \pm 2.1°$, $a = 4.02 \pm 0.1$ nm, and $b = 4.18 \pm 0.1$ nm.

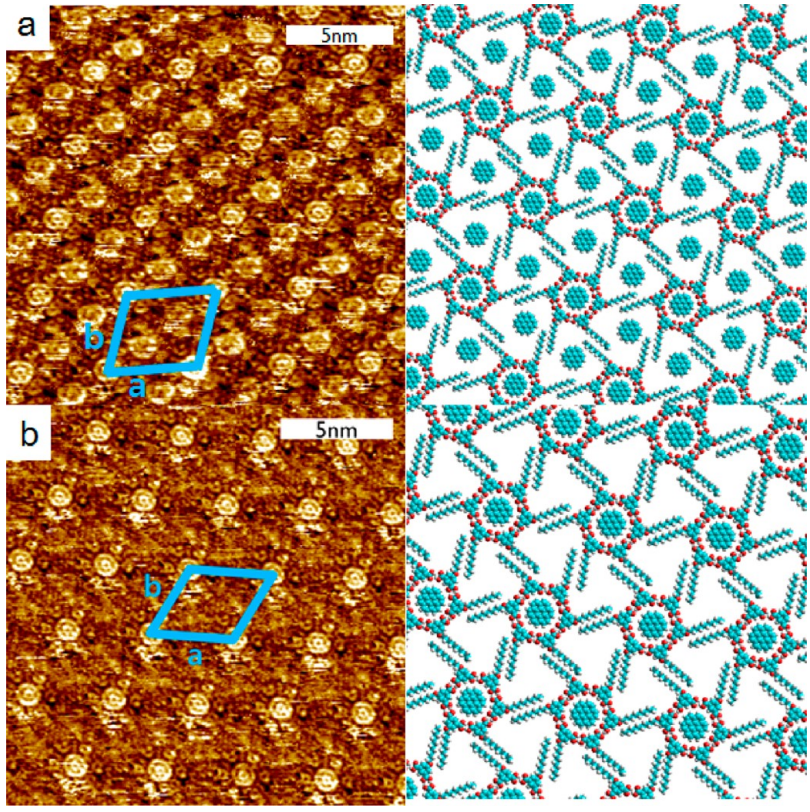

Figure 4. STM images and corresponding tentative molecular models of a premixture of COR and ISA-OC10 at (a) 1:10 ratio (0.10:0.98 mM COR/ISA-OC10; $V_{bias} = -0.65$ V; and $I_{set} = 0.12$ nA) and (b) 1:100 ratio (0.01:0.98 mM COR/ISA-OC10; $V_{bias} = -0.65$ V; and $I_{set} = 0.12$ nA). Unit cell parameters are (a) $\alpha = 75.6° \pm 1.0°$, $a = 2.94 \pm 0.2$ nm, and $b = 4.04 \pm 0.1$ nm; and (b) $\alpha = 61.7° \pm 0.6°$, $a = 3.67 \pm 0.1$ nm, and $b = 3.35 \pm 0.1$ nm.

dx.doi.org/10.1021/la5040849 | *Langmuir* 2014, 30, 15206−15211

appear as bright circular features within the hexagonal hydrogen-bonded pores of ISA. In the absence of COR but maintaining the same concentration of the ISA derivatives, the lamellar structure is the dominant polymorph. Therefore, COR not only acts as a guest molecule. Under conditions where ISA forms a lamellar structure, its presence forces the system to transform from a lamellar structure into the hexameric network. After closer inspection, it appears that for both ISA-OC18 and ISA-OC14 (panels b and c of Figure 3), the triangular pores are also accommodating COR molecules. In the case of ISA-OC18, the COR molecules inside the triangular pores appear as fuzzy features, while the COR molecules inside the hexagonal void are well-resolved, which can be correlated to the size mismatch between the triangular void and the adsorption of one COR molecule. On the basis of molecular modeling, a COR molecule adsorbed inside the triangular pore has the freedom to rotate and translate and the dynamic nature of COR adsorption into size-mismatched pores has been reported previously.[11] The COR molecules hosted inside the triangular pores of ISA-OC14, however, appear to be well-immobilized, and even though the triangular pore does not match the hexagonal shape of the COR molecule, the size matching appears to be sufficient to immobilize COR. In contrast, the presence of COR has a more dramatic effect on the hexameric structure of ISA-OC10. On the basis of molecular modeling, the triangular pore of ISA-OC10 would be too small for the co-adsorption of COR. COR addition, however, changes the hexameric patterns such that, within a hexamer of ISA-OC10, four of six alkyl chains are not interdigitated, thus creating additional empty space for the adsorption of COR. Within a unit cell, besides two triangular pores, each hosting a single COR molecule, a rhombic pore is created, which hosts two COR molecules (Figure 3a).

Because the presence of COR has an impact on the polymorph formation, it is not farfetched that the ratio of COR versus ISA could have an impact on the monolayer composition and architecture as well. This aspect was explored for ISA-OC10. Lowering the COR/ISA ratio gradually reduces the number of COR molecules adsorbed per unit cell. At a COR/ISA molar ratio of 1:10, a hexameric structure where all six alkyl chains are interdigitated is observed (Figure 4a). However, the alkyl chain interdigitation does not involve the whole end-to-end distance of adjacent alkyl chains, so that the triangular pore becomes large enough to host a single COR molecule. Finally, lowering the COR/ISA molar ratio to 1:100, COR adsorption only occurs in the hexagonal pores, while the triangular pores remain vacant (Figure 4b) and ideal alkyl chain interdigitation is restored. This illustrates the flexibility induced by the non-covalent van der Waals interactions; the ISA network reacts by expanding its pores to accommodate more COR, depending upon the specific COR/ISA ratio. This is reflected by the unit cell area, which increases from 10.9 nm^2 (1 COR molecule/unit cell) over 11.4 nm^2 (3 COR molecules/unit cell) to 14.0 nm^2 (5 COR molecules/unit cell) at COR/ISA ratios of 1:100, 1:10, and 1:1, respectively.

CONCLUSION

We have investigated the self-assembly properties of a series of alkylated ISA derivatives, which are governed by an interplay of van der Waals interactions and hydrogen bonds. These molecular building blocks can form two distinct polymorphs. It appears that the formation of these polymorphs is very sensitive to external variables. We have shown that it is possible to selectively form a specific network by varying the solute concentration, where a high concentration favors a high-density lamellar packing and a low concentration favors the formation of low-density porous networks. Moreover, we have demonstrated that a COR molecule is not only a suitable guest molecule to reside in the pores but may also induce a structural transformation from the lamellar packing to the porous network. Through a combination of these approaches, alkylated ISA derivatives become suitable building blocks to engineer a regular 2D nanoporous network, in which the distance between the pores can be tuned at will.

ASSOCIATED CONTENT

Supporting Information

Additional STM images of the self-assembly behavior of ISA-OC10 and ISA-OC18 with corresponding tentative molecular models. This material is available free of charge via the Internet at http://pubs.acs.org.

AUTHOR INFORMATION

Corresponding Authors

*E-mail: jinne.adisoejoso@chem.kuleuven.be.
*E-mail: steven.defeyter@chem.kuleuven.be.

Notes

The authors declare no competing financial interest.

ACKNOWLEDGMENTS

This work is supported by the Fund of Scientific Research—Flanders (FWO), KU Leuven (GOA 11/003), Belgian Federal Science Policy Office (IAP-7/05). Kwang-Won Park and Jongin Hong acknowledge the Basic Science Research Program (2013-026989) through the National Research Foundation (NRF) funded by the Ministry of Science, Information and Communications Technology (ICT) and Future Planning (MSIP) of Korea. Jinne Adisoejoso is a postdoctoral fellow of the FWO. This research has also received funding from the European Research Council under the European Union's Seventh Framework Programme (FP7/2007-2013)/ERC Grant Agreement 340324 as well as from DFG Priority Programme SPP 1459, ERC Grant on NANOGRAPH, Graphene Flagship (CNECT-ICT-604391), and European Union Projects UP-GRADE, GENIUS, and MoQuaS.

REFERENCES

(1) Ciesielski, A.; Palma, C.-A.; Bonini, M.; Samorì, P. Towards supramolecular engineering of functional nanomaterials: Pre-programming multi-component 2D self-assembly at solid−liquid interfaces. *Adv. Mater.* **2010**, *22* (32), 3506−3520.

(2) Mali, K. S.; Adisoejoso, J.; De Cat, I.; Balandina, T.; Ghijsens, E.; Guo, Z.; Li, M.; Sankara Pillai, M.; Vanderlinden, W.; Xu, H.; De Feyter, S. Physisorption for self-assembly of supramolecular systems: A scanning tunneling microscopy perspective. In *Supramolecular Chemistry*; John Wiley and Sons, Ltd.: Hoboken, NJ, 2012.

(3) Barth, J. V. Molecular architectonic on metal surfaces. *Annu. Rev. Phys. Chem.* **2007**, *58*, 375−407.

(4) Nath, K. G.; Ivasenko, O.; MacLeod, J. M.; Miwa, J. A.; Wuest, J. D.; Nanci, A.; Perepichka, D. F.; Rosei, F. Crystal engineering in two dimensions: An approach to molecular nanopatterning. *J. Phys. Chem. C* **2007**, *111* (45), 16996−17007.

(5) Pawin, G.; Wong, K. L.; Kwon, K.-Y.; Bartels, L. A homomolecular porous network at a Cu(111) surface. *Science* **2006**, *313* (5789), 961−962.

(6) Kampschulte, L.; Lackinger, M.; Maier, A. K.; Kishore, R. S. K.; Griessl, S.; Schmittel, M.; Heckl, W. M. Solvent induced poly-

morphism in supramolecular 1,3,5-benzenetribenzoic acid monolayers. *J. Phys. Chem. B* **2006**, *110* (22), 10829−10836.
(7) Stohr, M.; Wahl, M.; Galka, C. H.; Riehm, T.; Jung, T. A.; Gade, L. H. Controlling molecular assembly in two dimensions: The concentration dependence of thermally induced 2D aggregation of molecules on a metal surface. *Angew. Chem., Int. Ed.* **2005**, *44* (45), 7394−7398.
(8) Pawlak, R.; Clair, S.; Oison, V.; Abel, M.; Ourdjini, O.; Zwaneveld, N. A. A.; Gigmes, D.; Bertin, D.; Nony, L.; Porte, L. Robust supramolecular network on Ag(111): Hydrogen-bond enhancement through partial alcohol dehydrogenation. *ChemPhysChem* **2009**, *10* (7), 1032−1035.
(9) Xue, Y.; Zimmt, M. B. Patterned monolayer self-assembly programmed by side chain shape: Four-component gratings. *J. Am. Chem. Soc.* **2012**, *134* (10), 4513−4516.
(10) Zhang, X.; Chen, T.; Chen, Q.; Deng, G.-J.; Fan, Q.-H.; Wan, L.-J. One solvent induces a series of structural transitions in monodendron molecular self-assembly from lamellar to quadrangular to hexagonal. *Chem.—Eur. J.* **2009**, *15* (38), 9669−9673.
(11) Schull, G.; Douillard, L.; Fiorini-Debuisschert, C.; Charra, F.; Mathevet, F.; Kreher, D.; Attias, A. J. Selectivity of single-molecule dynamics in 2D molecular sieves. *Adv. Mater.* **2006**, *18* (22), 2954−2957.
(12) Tahara, K.; Lei, S.; Adisoejoso, J.; De Feyter, S.; Tobe, Y. Supramolecular surface-confined architectures created by self-assembly of triangular phenylene−ethynylene macrocycles via van der Waals interaction. *Chem. Commun.* **2010**, *46* (45), 8507−8525.
(13) Adisoejoso, J.; Li, Y.; Liu, J.; Liu, P. N.; Lin, N. Two-dimensional metallo-supramolecular polymerization: Toward size-controlled multistrand polymers. *J. Am. Chem. Soc.* **2012**, *134* (45), 18526−18529.
(14) Stepanow, S.; Lingenfelder, M.; Dmitriev, A.; Spillmann, H.; Delvigne, E.; Lin, N.; Deng, X. B.; Cai, C. Z.; Barth, J. V.; Kern, K. Steering molecular organization and host−guest interactions using two-dimensional nanoporous coordination systems. *Nat. Mater.* **2004**, *3* (4), 229−233.
(15) Lingenfelder, M. A.; Spillmann, H.; Dmitriev, A.; Stepanow, S.; Lin, N.; Barth, J. V.; Kern, K. Towards surface-supported supramolecular architectures: Tailored coordination assembly of 1,4-benzenedicarboxylate and Fe on Cu(100). *Chem.—Eur. J.* **2004**, *10* (8), 1913−1919.
(16) Lei, S.; Tahara, K.; De Schryver, F. C.; Van der Auweraer, M.; Tobe, Y.; De Feyter, S. One building block, two different supramolecular surface-confined patterns: Concentration in control at the solid−liquid interface. *Angew. Chem., Int. Ed.* **2008**, *47* (16), 2964−2968.
(17) Kampschulte, L.; Werblowsky, T. L.; Kishore, R. S. K.; Schmittel, M.; Heckl, W. M.; Lackinger, M. Thermodynamical equilibrium of binary supramolecular networks at the liquid−solid interface. *J. Am. Chem. Soc.* **2008**, *130* (26), 8502−8507.
(18) Tahara, K.; Furukawa, S.; Uji-i, H.; Uchino, T.; Ichikawa, T.; Zhang, J.; Mamdouh, W.; Sonoda, M.; De Schryver, F. C.; De Feyter, S.; Tobe, Y. Two-dimensional porous molecular networks of dehydrobenzo[12]annulene derivatives via alkyl chain interdigitation. *J. Am. Chem. Soc.* **2006**, *128* (51), 16613−16625.
(19) Palma, C.-A.; Bonini, M.; Llanes-Pallas, A.; Breiner, T.; Prato, M.; Bonifazi, D.; Samori, P. Pre-programmed bicomponent porous networks at the solid-liquid interface: The low concentration regime. *Chem. Commun.* **2008**, *42*, 5289−5291.
(20) Ahn, S.; Matzger, A. J. Six different assemblies from one building block: Two-dimensional crystallization of an amide amphiphile. *J. Am. Chem. Soc.* **2010**, *132* (32), 11364−11371.
(21) Blunt, M. O.; Adisoejoso, J.; Tahara, K.; Katayama, K.; Van der Auweraer, M.; Tobe, Y.; De Feyter, S. Temperature-induced structural phase transitions in a two-dimensional self-assembled network. *J. Am. Chem. Soc.* **2013**, *135* (32), 12068−12075.
(22) Adisoejoso, J.; Tahara, K.; Lei, S.; Szabelski, P.; Rżysko, W.; Inukai, K.; Blunt, M. O.; Tobe, Y.; De Feyter, S. One building block, two different nanoporous self-assembled monolayers: A combined STM and Monte Carlo study. *ACS Nano* **2011**, *6* (1), 897−903.
(23) Marie, C.; Silly, F.; Tortech, L.; Müllen, K.; Fichou, D. Tuning the packing density of 2D supramolecular self-assemblies at the solid−liquid interface using variable temperature. *ACS Nano* **2010**, *4* (3), 1288−1292.
(24) Gutzler, R.; Sirtl, T.; Dienstmaier, J. F.; Mahata, K.; Heckl, W. M.; Schmittel, M.; Lackinger, M. Reversible phase transitions in self-assembled monolayers at the liquid−solid interface: Temperature-controlled opening and closing of nanopores. *J. Am. Chem. Soc.* **2010**, *132* (14), 5084−5090.
(25) Bellec, A.; Arrigoni, C.; Schull, G.; Douillard, L.; Fiorini-Debuisschert, C.; Mathevet, F.; Kreher, D.; Attias, A.-J.; Charra, F. Solution-growth kinetics and thermodynamics of nanoporous self-assembled molecular monolayers. *J. Chem. Phys.* **2011**, *134* (12), 124702−7.
(26) Yang, Y.; Wang, C. Solvent effects on two-dimensional molecular self-assemblies investigated by using scanning tunneling microscopy. *Curr. Opin. Colloid Interface Sci.* **2009**, *14* (2), 135−147.
(27) Yibao, L.; Zhun, M.; Guicun, Q.; Yanlian, Y.; Qingdao, Z.; Xiaolin, F.; Chen, W.; Wei, H. Solvent effects on supramolecular networks formed by racemic star-shaped oligofluorene studied by scanning tunneling microscopy. *J. Phys. Chem. C* **2008**, *112* (23), 8649−53.
(28) De Feyter, S.; Gesquière, A.; Klapper, M.; Müllen, K.; De Schryver, F. C. Toward two-dimensional supramolecular control of hydrogen-bonded arrays: The case of isophthalic acids. *Nano Lett.* **2003**, *3* (11), 1485−1488.
(29) Dickerson, P. N.; Hibberd, A. M.; Oncel, N.; Bernasek, S. L. Hydrogen-bonding versus van der Waals interactions in self-assembled monolayers of substituted isophthalic acids. *Langmuir* **2010**, *26* (23), 18155−18161.
(30) Bernasek, S. L.; Feng, T. Self-assembly of 5-octadecyloxyisophthalic acid and its coadsorption with terephthalic acid. *Surf. Sci.* **2007**, *601* (10), 2284−90.
(31) Furukawa, S.; Tahara, K.; De Schryver, F. C.; Van der Auweraer, M.; Tobe, Y.; De Feyter, S. Structural transformation of a two-dimensional molecular network in response to selective guest inclusion. *Angew. Chem., Int. Ed.* **2007**, *46* (16), 2831−2834.
(32) Griessl, S.; Lackinger, M.; Edelwirth, M.; Hietschold, M.; Heckl, W. M. Self-assembled two-dimensional molecular host−guest architectures from trimesic acid. *Single Mol.* **2002**, *3* (1), 25−31.
(33) These orientations are observed randomly throughout a series of adjacent lamella; therefore, unit cell parameters were not calculated.
(34) Lei, S.; Surin, M.; Tahara, K.; Adisoejoso, J.; Lazzaroni, R.; Tobe, Y.; Feyter, S. D. Programmable hierarchical three-component 2D assembly at a liquid−solid interface: Recognition, selection, and transformation. *Nano Lett.* **2008**, *8* (8), 2541−2546.
(35) The specific intermolecular interactions between solvent and ISA molecules or mutual solvent molecules at play remain unknown.
(36) The concentration range probed for ISA-OC10 is limited by its solubility.
(37) Blunt, M. O.; Russell, J. C.; Champness, N. R.; Beton, P. H. Templating molecular adsorption using a covalent organic framework. *Chem. Commun.* **2010**, *46* (38), 7157−7159.
(38) Li, Y.; Ma, Z.; Deng, K.; Lei, S.; Zeng, Q.; Fan, X.; De Feyter, S.; Huang, W.; Wang, C. Thermodynamic controlled hierarchical assembly of ternary supramolecular networks at the liquid−solid interface. *Chem.—Eur. J.* **2009**, *15* (22), 5418−5423.
(39) Lackinger, M.; Heckl, W. M. Carboxylic acids: Versatile building blocks and mediators for two-dimensional supramolecular self-assembly. *Langmuir* **2009**, *25* (19), 11307−11321.